

Short Communication

## Co-sintering synthesis of Yb<sup>3+</sup> and Sm<sup>3+</sup> co-doped CeO<sub>2</sub>/NiO composite as a solid electrolyte and its electrochemical properties

Zhuang Fu, Shouyue Wang, Yan Zheng, Wenxuan Pan, Jie Liu\*, Hongtao Wang\*, Qingmei Guan\*

Anhui Provincial Key Laboratory for Degradation and Monitoring of Pollution of the Environment; School of Chemical and Material Engineering, Fuyang Normal University, Fuyang 236037, China

\*E-mail: [200107008@fynu.edu.cn](mailto:200107008@fynu.edu.cn); [200707049@fynu.edu.cn](mailto:200707049@fynu.edu.cn)

Received: 24 February 2022 / Accepted: 21 March 2022 / Published: 5 April 2022

In this study, Ce<sub>0.8</sub>Yb<sub>0.1</sub>Sm<sub>0.1</sub>O<sub>2-α</sub> was synthesized using a citric acid-nitrate combustion method. Ce<sub>0.8</sub>Yb<sub>0.1</sub>Sm<sub>0.1</sub>O<sub>2-α</sub>-4 mol% NiO (CYSO-NiO) was also obtained using the 800 °C CYSO powder uniformly mixed with 4 mol% NiO. The phases and microstructures of CYSO and CYSO-NiO were analysed by an X-ray diffractometer (XRD) and a scanning electron microscope (SEM). XRD spectra indicated that the addition of 4 mol% NiO had no effect on the crystal structure of CYSO. The conductivities of CYSO and CYSO-NiO were 2.7×10<sup>-2</sup> S·cm<sup>-1</sup> and 5.6×10<sup>-2</sup> S·cm<sup>-1</sup> at 750 °C, respectively. The maximum output power densities of CYSO and CYSO-NiO were 44.1 mW·cm<sup>-2</sup> and 46.6 mW·cm<sup>-2</sup> at 750 °C, respectively.

**Keywords:** Electrolyte; Fuel cell; CeO<sub>2</sub>; Conductivity

### 1. INTRODUCTION

Traditional energy power generation needs multiple energy conversions, which are limited by the thermodynamic Carnot cycle. Fuel cells can directly convert chemical energy into electrical energy, which is not limited by the thermodynamic Carnot cycle theoretically. A solid oxide fuel cell (SOFC) is a kind of all solid fuel cell, which avoids the problem of corrosion of a liquid electrolyte [1-6]. In 1937, the first SOFC with zirconia as the electrolyte was developed. Due to the high working temperature (800–1000 °C), the battery had some problems in the working process. In order to reduce the working temperature of these batteries, the development of materials with high ionic conductivities at medium temperature (600–800 °C) has become a research hotspot [7-11].

CeO<sub>2</sub>-based electrolytes are intermediate-temperature electrolytes widely studied at present. The ionic conductivities of CeO<sub>2</sub>-based electrolytes can be improved by doping some low valence metal

oxides [12-16]. Dai *et al.* assembled a SOFC using  $\text{Ce}_{0.8}\text{Sm}_{0.2}\text{O}_{2-\alpha}$  as the electrolyte by a co-firing method [15]. The researchers also co-doped two or more metal oxides to  $\text{CeO}_2$  to obtain higher ion conductivities and long-time stabilities [17-22]. Vijaykumar *et al.* prepared  $\text{Ce}_{0.85}\text{Ln}_{0.10}\text{Sr}_{0.05}\text{O}_{2-\delta}$  (Ln = La and Gd) electrolytes using a nitrate-sucrose combustion method [19]. The conductivities of  $\text{Ce}_{0.85}\text{Gd}_{0.10}\text{Sr}_{0.05}\text{O}_{2-\delta}$  and  $\text{Ce}_{0.85}\text{La}_{0.10}\text{Sr}_{0.05}\text{O}_{2-\delta}$  were  $6.78 \times 10^{-3} \text{ S}\cdot\text{cm}^{-1}$  and  $2.72 \times 10^{-3} \text{ S}\cdot\text{cm}^{-1}$  at 600 °C, respectively.

A uniform nanometre powder can be obtained by the liquid phase method. Compared with coprecipitation and hydrothermal synthesis, the nitrate combustion process is simple, and there is no ion loss and cation ratio mismatch in the preparation process [23-24]. Therefore, this paper chooses the nitrate combustion method to prepare the powder. NiO is one of the most commonly used sintering aids, which can effectively reduce the sintering temperature of  $\text{CeO}_2$  based electrolyte materials.

Therefore,  $\text{Ce}_{0.8}\text{Yb}_{0.1}\text{Sm}_{0.1}\text{O}_{2-\alpha}$  was synthesized using a citric acid-nitrate combustion method in this paper. And we tried to improve the structure and properties of  $\text{Ce}_{0.8}\text{Yb}_{0.1}\text{Sm}_{0.1}\text{O}_{2-\alpha}$  by adding sintering assistant NiO.

## 2. EXPERIMENTAL

Firstly,  $\text{Ce}_{0.8}\text{Yb}_{0.1}\text{Sm}_{0.1}\text{O}_{2-\alpha}$  was synthesized using a citric acid-nitrate combustion method. Analytical pure  $\text{Yb}_2\text{O}_3$ ,  $\text{Sm}_2\text{O}_3$  and ammonium ceric nitrate were dissolved and dispersed in distilled water and concentrated nitric acid solution, respectively, according to the stoichiometric ratios. The fuel citric acid was then added to the solution and heated until spontaneous combustion.  $\text{Ce}_{0.8}\text{Yb}_{0.1}\text{Sm}_{0.1}\text{O}_{2-\alpha}$  (CYSO) was obtained after being calcinated at 800 °C and 1450 °C for 5 h, respectively.  $\text{Ce}_{0.8}\text{Yb}_{0.1}\text{Sm}_{0.1}\text{O}_{2-\alpha}$ -4 mol% NiO (CYSO-NiO) was obtained after sintering at 1450 °C for 5 h using the 800 °C CYSO powder uniformly mixed with 4 mol% NiO.

The phases of the synthesized powders were analysed by XRD. The microstructures of CYSO and CYSO-NiO sintered samples were observed by a scanning electron microscope (SEM). The electrical conductivities of the CYSO and CYSO-NiO sintered samples in air atmosphere were measured by AC impedance spectroscopy. The oxygen concentration discharge cell:  $\text{O}_2$ , Pd-Ag|electrolyte|Pd-Ag, air and  $\text{H}_2/\text{O}_2$  fuel cell performances of CYSO and CYSO-NiO at 750 °C were also studied.

## 3. RESULTS AND DISCUSSION

Fig. 1 shows the XRD spectra of the 800 °C CYSO powder, 1450 °C CYSO and CYSO-NiO sintered samples, respectively. In addition to the diffraction peaks of  $\text{CeO}_2$ , there are very few rare earth oxide phases in 800 °C CYSO. This indicates that the initial firing temperature should continue to increase appropriately. The half peak width of 800 °C CYSO indicates that the grain size is on the nanometre scale. It can be seen from Fig. 1 that the 1450 °C CYSO and CYSO-NiO sintered samples have a single fluorite structure [16-18]. CYSO-NiO is a single cubic fluorite phase, indicating that the addition of 4 mol% NiO has no effect on the crystal structure of CYSO [25].

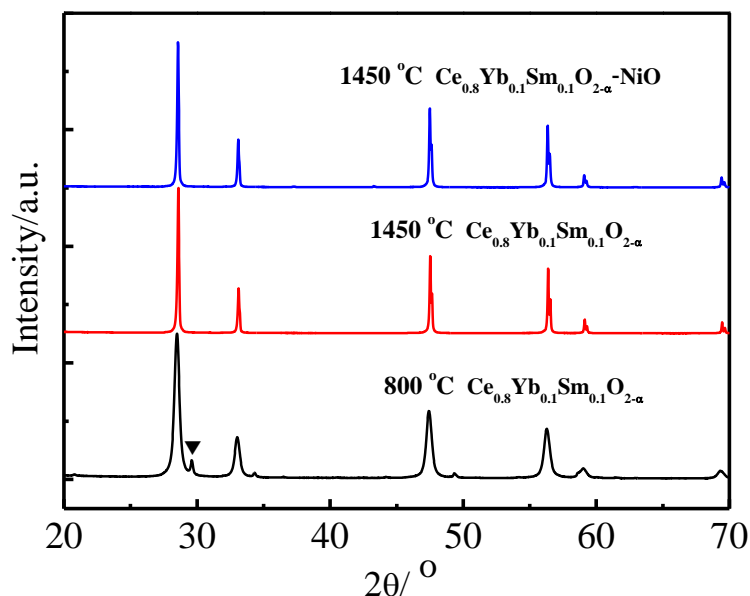


**Figure 1.** XRD spectra of 800 °C CYSO powder, 1450 °C CYSO and CYSO-NiO sintered samples, respectively.

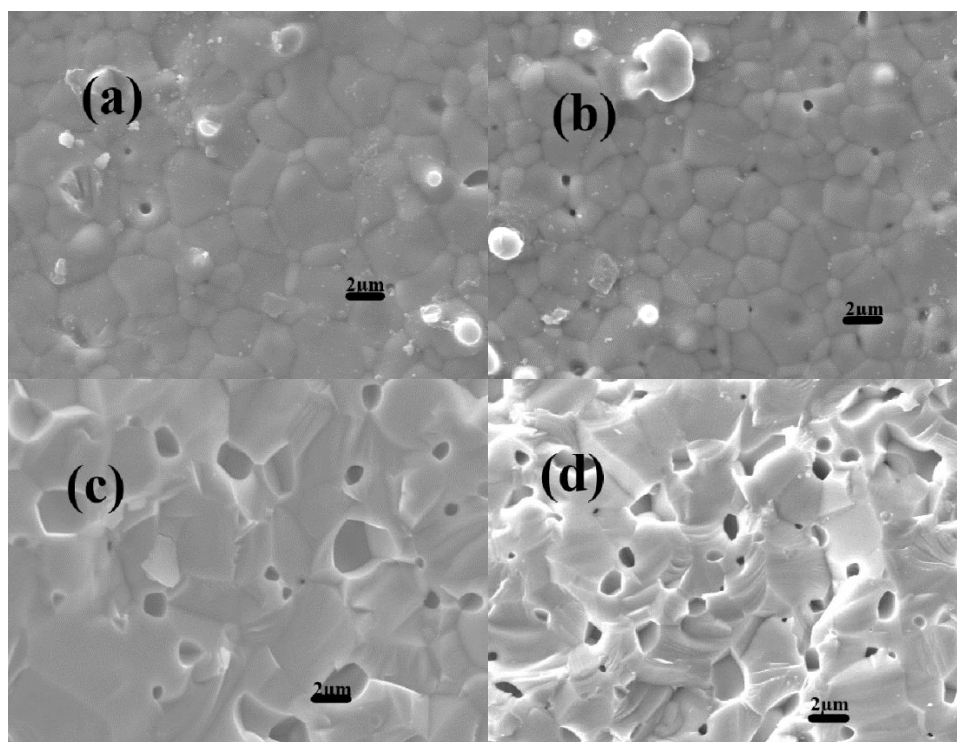


**Figure 2.** SEM photos of surface and cross section of CYSO (a, c) and CYSO-NiO (b, d) sintered samples.

Fig. 2 shows the SEM photos of the surface and cross section of the CYSO (a, c) and CYSO-NiO (b, d) sintered samples. As can be seen from Fig. 2(a, b), the surface microstructures of CYSO and CYSO-NiO are relatively dense. The grain sizes of CYSO (2-4 μm) and CYSO-NiO (1.5-3 μm) can be obtained by measurement. This may be due to the distribution of sintering additive NiO between grain boundaries, which delays the grain polymerization of CYSO. From Fig. 2(c and d), the cross-section microstructures of CYSO and CYSO-NiO have a small number of closed pores. The samples have high

compactness and meet the test requirements. At present, a reasonable explanation is that the low melting point of added NiO leads to the acceleration of grain rearrangement during sintering [23-25].

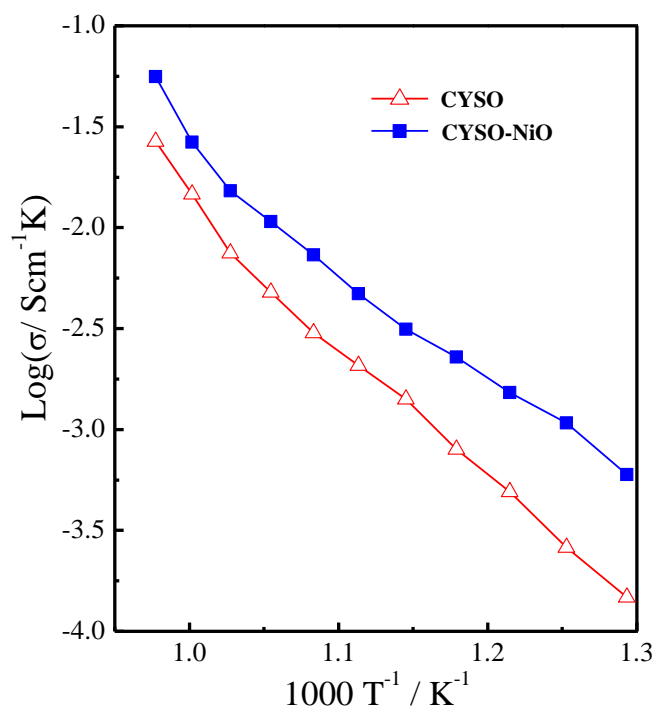


**Figure 3.** The  $\log \sigma \sim 1000 T^{-1}$  plots of CYSO and CYSO-NiO sintered samples at 500-750 °C in air atmosphere.

**Table 1.** The conductivities of CYSO, CYSO-NiO and  $M^{n+}$ -doped  $CeO_2$  in the literatures.

solid electrolytes	conductivities ( $10^{-2} S \cdot cm^{-1}$ )			
	600 °C	650 °C	700 °C	750 °C
CYSO			0.75	2.7
CYSO-NiO		0.73	1.6	5.6
$Ce_{0.8}Sm_{0.1}Ba_{0.05}Er_{0.05}O_{2-\alpha}$		0.38	0.64	1.2 [26]
$Ce_{0.8}Sm_{0.2}O_{2-\alpha}$ -30% $Al_2O_3$	0.32	0.67 [27]		

The Arrhenius plots of CYSO and CYSO-NiO sintered samples at 500-750 °C in air atmosphere are shown in Fig. 3. It can be seen from Fig. 3 that the ionic conductivities of CYSO and CYSO-NiO increased rapidly with the increase of temperature. The conductivity of CYSO was  $1.4 \times 10^{-3} S \cdot cm^{-1}$  at 600 °C, which was lower than those Vijaykumar *et al.* reported for  $Ce_{0.85}La_{0.10}Sr_{0.05}O_{2-\delta}$  ( $2.72 \times 10^{-3} S \cdot cm^{-1}$ ) at 600 °C. However, the conductivity of CYSO-NiO was  $3.2 \times 10^{-3} S \cdot cm^{-1}$  at 600 °C, which was higher than for CYSO. This may be due to the improvement of grain boundary conductivity by NiO which promotes the rapid increase of conductivity. And the conductivities of CYSO and CYSO-NiO were  $2.7 \times 10^{-2} S \cdot cm^{-1}$  and  $5.6 \times 10^{-2} S \cdot cm^{-1}$  at 750 °C, respectively. Table 1 shows the conductivities of CYSO,

CYSO-NiO and  $M^{n+}$ -doped  $CeO_2$  found in the literatures. The conductivities of  $Sm^{3+}$ ,  $Er^{3+}$  and  $Ba^{2+}$  co-doped  $Ce_{0.8}Sm_{0.1}Ba_{0.05}Er_{0.05}O_{2-\alpha}$  reach  $3.8 \times 10^{-3} S \cdot cm^{-1}$ ,  $6.4 \times 10^{-3} S \cdot cm^{-1}$  and  $1.2 \times 10^{-2} S \cdot cm^{-1}$  at 650 °C, 700 °C and 750 °C, respectively [26]. The conductivities of 20 mol% samarium doped ceria/alumina composite electrolyte are  $3.2 \times 10^{-3} S \cdot cm^{-1}$  and  $6.7 \times 10^{-3} S \cdot cm^{-1}$  at 600 °C and 650 °C, respectively [27]. At the same test temperature, the conductivity of CYSO is higher than  $Ce_{0.8}Sm_{0.1}Ba_{0.05}Er_{0.05}O_{2-\alpha}$  and that of CYSO-NiO is much higher than  $Ce_{0.8}Sm_{0.2}O_{2-\alpha}-30\%Al_2O_3$ . The conductivities of CYSO-NiO are 2.1 times higher than that of CYSO. This shows that adding an appropriate amount of NiO can reduce the space charge and the blocking effect of the grain boundary, which is conducive to the improvement of conductivity.

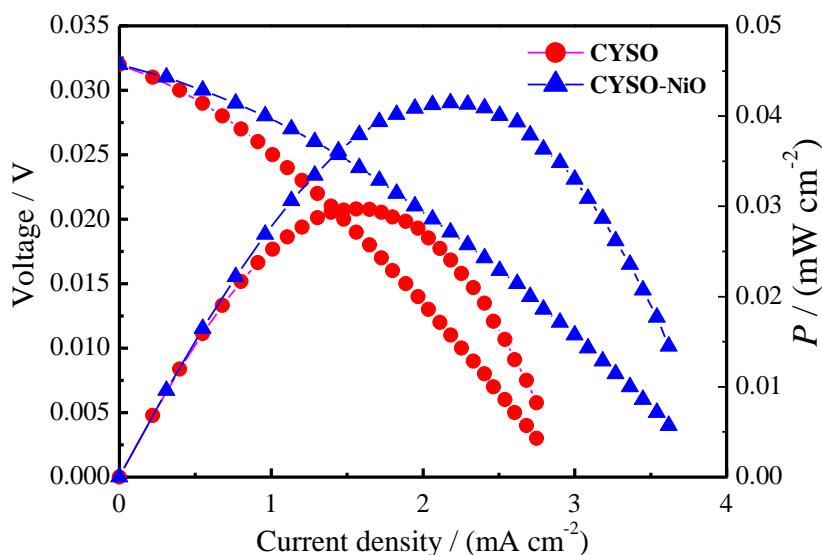


**Figure 4.** The oxygen concentration discharge cells:  $O_2$ , Pd-Ag|electrolyte|Pd-Ag, air of CYSO and CYSO-NiO at 750 °C.

Fig. 4 shows the oxygen concentration discharge cells:  $O_2$ , Pd-Ag|electrolyte|Pd-Ag, air of CYSO and CYSO-NiO at 750 °C. As can be seen from Fig. 4, with the increase of discharge current density, the power density first decreases and then increases. There is a continuous and stable discharge curve, indicating that there are conductive ions that can continuously move directionally. Metal ions cannot continue, only oxygen ions conduct directionally in an oxidizing atmosphere. The open circuit voltages of the oxygen concentration discharge cells are close to the theoretical electromotive force. Therefore, the conductivities in air in Fig. 3 can be regarded as oxide ionic conductivities.

Fig. 5 shows the  $I$ - $V$ - $P$  curves of  $H_2/O_2$  fuel cells using CYSO and CYSO-NiO as electrolytes at 750 °C. The open circuit voltages of CYSO and CYSO-NiO are maintained at 0.98–1.02 V because the activity of oxide ions in the electrolytes are greatly enhanced and the catalytic activity of the electrode is improved at 750 °C. The open circuit voltages are lower than the theoretical values, indicating that a small amount of  $Ce^{4+}$  is reduced to  $Ce^{3+}$  in an anodic reducing atmosphere. The output power densities increase with the increase of working current densities. When certain working current densities are

reached, the output power densities reach the maximum. The maximum output power densities of CYSO and CYSO-NiO are  $44.1 \text{ mW}\cdot\text{cm}^{-2}$  and  $46.6 \text{ mW}\cdot\text{cm}^{-2}$  at  $750 \text{ }^\circ\text{C}$ , respectively.

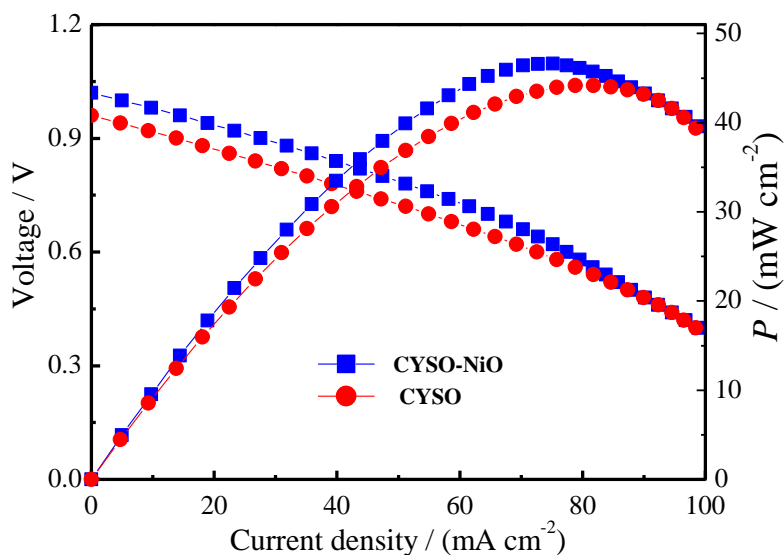


**Figure 5.** The  $I$ - $V$ - $P$  curves of  $\text{H}_2/\text{O}_2$  fuel cells using CYSO and CYSO-NiO as electrolytes at  $750 \text{ }^\circ\text{C}$ .

#### 4. CONCLUSIONS

In this study, CYSO and CYSO-NiO was synthesized at  $1450 \text{ }^\circ\text{C}$ . SEM results showed that the addition of NiO led to the acceleration of grain rearrangement during sintering. The oxygen concentration discharge cells indicated that there are oxide ionic conductivities in an oxidizing atmosphere. The maximum output power densities of CYSO and CYSO-NiO are  $44.1 \text{ mW}\cdot\text{cm}^{-2}$  and  $46.6 \text{ mW}\cdot\text{cm}^{-2}$  at  $750 \text{ }^\circ\text{C}$ , respectively.

#### ACKNOWLEDGEMENTS

This work was supported by the National Natural Science Foundation (21807012) of China. Scientific research projects for college students of Fuyang Normal University (XSKY2021-LG028).

#### CONFLICTS OF INTEREST

The authors declare no conflicts of interest.

#### References

1. H. Jiang and F. Zhang, *Int. J. Electrochem. Sci.*, 15 (2020) 959.
2. T. Hibino, K. Kobayashi, S. Teranishi and T. Hitomi, *ACS Sust. Chem. Eng.*, 9 (2021) 3124.
3. Y. Liu, P. Liu, J. Ren, Z. Jin and X. Han, *Int. J. Electrochem. Sci.*, 17 (2022) 220319.
4. S. Kim, G. Kim and A. Manthiram, *J. Power Sources*, 497 (2021) 229873.
5. J. Zhao, Q. Liang, Y. Liang and J. Hu, *Int. J. Electrochem. Sci.*, 17 (2022) 220313.
6. Z.Y. Zhang, D.T. Xie, J.P. Ni and C.S. Ni, *Ceram. Int.*, 47 (2021) 14673.
7. D. Dai, Y. Liu, H. Qiu, D. Xiao and H. Jiang, *Int. J. Electrochem. Sci.*, 17 (2022) 220231.

8. Q. Ji, L. Bi, J. Zhang, H. Cao and X. Zhao, *Energ. Environ. Sci.*, 13 (2020) 1408.
9. D.A. Osinkin, *Electrochim. Acta*, 372 (2021) 137858.
10. M.R. Kosinski and R.T. Baker, *J. Power Sources*, 196 (2011) 2498.
11. W. Zhang, T. Hu, R. Shi and H. Wang, *Int. J. Electrochem. Sci.*, 15 (2020) 304.
12. L. dos Santos-Gómez, J. Zamudio-García, J.M. Porras-Vázquez, E.R. Losilla and D. Marrero-López, *J. Eur. Ceram. Soc.*, 40 (2020) 3080.
13. A. Arabaci, *Mater. Res.*, 9 (2020) 296.
14. X. Sun, T. Wang, D. Yan, G. Zhang, D. Wang, C. Wang and R. Liu, *Ceram. Int.*, 46 (2020) 7218.
15. H. Dai, H. Kou, Z. Tao, K. Liu, M. Xue, Q. Zhang and L. Bi, *Ceram. Int.*, 46 (2020) 6987.
16. Z. Huang, L. Fan, N. Hou, T. Gan, J. Gan, Y. Zhao and Y. Li, *J. Power Sources*, 451 (2020) 227809.
17. Y. Xue, S. An, S. Li, J. Peng, C. Cai and Y. Liu, *J. Solid State Electr.*, 24 (2020) 1639.
18. H. Lv, Z. Gong, Y. Xia, Z. Jin, D. Wang and W. Liu, *Ceram. Int.*, 46 (2020) 10379.
19. V. Vijaykumar, G. Nirala, D. Yadav, U. Kumar and S. Upadhyay, *Int. J. Energy Res.*, 44 (2020) 4652.
20. A. Arabaci, *Mater. Sci. Eng. B*, 260 (2020) 114646.
21. F. Altaf, R. Batool, R. Gill, G. Abbas, R. Raza, M.A. Khan, Zohaib-ur Rehman and M.A. Ahmad, *Ceram. Int.*, 45 (2019) 10330.
22. S. Shirbhate, R. N. Nayyar, P. K. Ojha, A. K. Yadav and S. Acharya, *J. The Electrochem. Soc.*, 166 (2019) F544.
23. N. Tian, Y. Qu, H. Men, J. Yu, X. Wang and J. Zheng, *Solid State Ionics*, 351 (2020) 115331.
24. S. Preethi, M. Abhiroop and K. Suresh Babu, *Ceram. Int.*, 45 (2019) 5819.
25. J. Cheng, C. Tian and J. Yang, *J. Mater. Sci.: Mater. El.*, 30 (2019) 16613.
26. A.S.A Muhammed, M. Anwar and A.M. Abdalla, *Ceram. Int.*, 43 (2017) 1265.
27. Q. Yang, B. Meng and Z. Lin, *J. Am. Ceram. Soc.*, 100 (2017) 686.